Journal of Theoretical Biology 394 (2016) 212–222

Contents lists available at ScienceDirect

Journal of Theoretical Biology

journal homepage: www.elsevier.com/locate/yjtbi

A network model for Ebola spreading

Alessandro Rizzo [a,b,*], Biagio Pedalino [c], Maurizio Porfiri [a,*]

[a] New York University, Tandon School of Engineering, Department of Mechanical and Aerospace Engineering, Six MetroTech Center, Brooklyn, NY 11201, USA
[b] Politecnico di Torino, Dipartimento di Automatica e Informatica, Corso Duca degli Abruzzi 24, 10129 Torino, Italy
[c] TEPHINET (Training Programs in Epidemiology and Public Health Interventions Network) in Cooperative Agreement with the Workforce and Institutions Development Branch at the Center for Global Health of the Centers for Disease Control and Prevention, Atlanta, GA30329, USA

HIGHLIGHTS

- We define a realistic Ebola model that does not rely on homogeneous mixing.
- We reproduce the dynamics of the 2014–2015 Ebola outbreak in Liberia.
- We model non-ideal and time-varying intervention policies.
- We assess the efficacy intervention policies with respect to their application time.

ARTICLE INFO

Article history:
Received 10 June 2015
Received in revised form
18 December 2015
Accepted 12 January 2016
Available online 21 January 2016

Keywords:
Activity driven networks
Ebola virus disease
Epidemic model
Interventions
Liberia

ABSTRACT

The availability of accurate models for the spreading of infectious diseases has opened a new era in management and containment of epidemics. Models are extensively used to plan for and execute vaccination campaigns, to evaluate the risk of international spreadings and the feasibility of travel bans, and to inform prophylaxis campaigns. Even when no specific therapeutical protocol is available, as for the Ebola Virus Disease (EVD), models of epidemic spreading can provide useful insight to steer interventions in the field and to forecast the trend of the epidemic. Here, we propose a novel mathematical model to describe EVD spreading based on activity driven networks (ADNs). Our approach overcomes the simplifying assumption of homogeneous mixing, which is central to most of the mathematically tractable models of EVD spreading. In our ADN-based model, each individual is not bound to contact every other, and its network of contacts varies in time as a function of an activity potential. Our model contemplates the possibility of non-ideal and time-varying intervention policies, which are critical to accurately describe EVD spreading in afflicted countries. The model is calibrated from field data of the 2014 April-to-December spreading in Liberia. We use the model as a predictive tool, to emulate the dynamics of EVD in Liberia and offer a one-year projection, until December 2015. Our predictions agree with the current vision expressed by professionals in the field, who consider EVD in Liberia at its final stage. The model is also used to perform a what-if analysis to assess the efficacy of timely intervention policies. In particular, we show that an earlier application of the same intervention policy would have greatly reduced the number of EVD cases, the duration of the outbreak, and the infrastructures needed for the implementation of the intervention.

1. Introduction

Since the discovery of Ebola viruses in 1976, the 2014–2015 outbreak of the Ebola Virus Disease (EVD) has been the largest in terms of number of countries involved, reported cases, and casualties. As of December 13, 2015 the Centers for Disease Control and Prevention (CDC) have reported more than 28,600 cases in six West African countries, of which about 15,200 have been laboratory confirmed, totaling more than 11,300 casualties (Centers for Disease Control and Prevention, 2014a). Outside of these regions, one case has been reported in Spain, one in the United Kingdom, and four in the United States of America, one of which has resulted in a casualty (Centers for Disease Control and Prevention, 2014b). While massive interventions are currently underway in afflicted countries, unaffected countries worldwide are striving to strengthen their preparedness and response plans through clinical

* Corresponding authors at: New York University, Tandon School of Engineering, Department of Mechanical and Aerospace Engineering, Six MetroTech Center, Brooklyn, NY 11201, USA.
E-mail addresses: alessandro.rizzo@nyu.edu (A. Rizzo), pedalinobiagio@gmail.com (B. Pedalino), mporfiri@nyu.edu (M. Porfiri).

http://dx.doi.org/10.1016/j.jtbi.2016.01.015
0022-5193/

and non-clinical interventions (Centers for Disease Control and Prevention, 2014c). In this context, mathematical modeling of infectious disease spreading can provide paramount information on the progression of EVD and on short/long-term outcomes of the epidemics. At the same time, policy makers could benefit from quantitative and qualitative information afforded by such mathematical models that directly assess the effectiveness of intervention policies (Keeling and Eames, 2005; Legrand et al., 2007; Brauer and Castillo-Chavez, 2011; Keeling and Rohani, 2011; Althaus, 2014; Fisman et al., 2014; Gomes et al., 2014; Meltzer et al., 2014; Nishiura and Chowell, 2014; Rivers et al., 2014; Towers et al., 2014; Merler et al., 2015; Valdez et al., 2015; Webb et al., 2015).

As in the study of many other infectious diseases (Keeling and Eames, 2005; Brauer and Castillo-Chavez, 2011; Keeling and Rohani, 2011), modeling efforts on EVD have mainly focused on mean-field compartmental models, either deterministic or stochastic, and agent-based models (Chowell et al., 2004; Althaus, 2014; CDC Stacks, 2014; Fasina et al., 2014; Fisman et al., 2014; Gomes et al., 2014; Kiskowski, 2014; Lewnard et al., 2014; Meltzer et al., 2014; Nishiura and Chowell, 2014; Pandey et al., 2014; Poletto et al., 2014; Rivers et al., 2014; Towers et al., 2014; Merler et al., 2015; Valdez et al., 2015; Webb et al., 2015). Although these models are valuable tools for simulation and prediction of EVD scenarios, they suffer from limitations that reduce their capability to accurately-and-quickly assess the effectiveness of specific intervention policies and pathways for their improvement.

Mean-field compartmental models are based on deterministic or stochastic differential equations, in which relevant variables, called compartments, evolve in time to describe the fraction of the population in a given state of the epidemic model (Brauer and Castillo-Chavez, 2011; Keeling and Rohani, 2011). Several mean-field compartmental models have been recently formulated to describe the spreading of EVD and assess the impact of non-pharmaceutical interventions (Chowell et al., 2004; Althaus, 2014; CDC Stacks, 2014; Fasina et al., 2014; Fisman et al., 2014; Kiskowski, 2014; Lewnard et al., 2014; Meltzer et al., 2014; Nishiura and Chowell, 2014; Pandey et al., 2014; Rivers et al., 2014; Towers et al., 2014; Webb et al., 2015). These models are usually calibrated through least-squares optimization on available epidemic data (World Health Organization, 2014a). Then, several instances of the model are studied, varying one or more parameters, to anticipate plausible scenarios for the evolution of the outbreak in terms of the total number of infections and casualties.

Mean-field approximations are effective to enable a first, mathematically rigorous understanding of EVD spreading, but suffer from several limitations. While these models are computationally simple and theoretically tractable, they do not take into account the inherently time-varying nature of human behavior, which is influenced by several factors, such as health status or risk perception (Ferguson, 2007; Funk et al., 2010; Manfredi and D'Onofrio, 2013). In their basic incarnation, they rely on the assumption of homogeneous mixing, whereby each individual contacts every other. This assumption typically yields an overestimation of cases (Lewnard et al., 2014; Merler et al., 2015), since social interactions in populations are heterogeneous in both number and intensity (Barrat et al., 2008; Holme and Saramäki, 2012; Perra and Goncalves, 2015). Although heterogeneities could be included by refining and increasing the spectrum of compartments (Brauer, 2008; Choe and Lee, 2015), such an approach may challenge rigorous analytical treatment and parameter identification.

On the opposite side of the spectrum from mean-field compartmental models in terms of complexity are agent-based models. These models are based on the stochastic simulation of individuals' motion and interaction, following specific rules, spatial constraints, and mobility patterns (Ajelli et al., 2010). A comprehensive agent-based model for worldwide simulation, the Global Epidemic and Mobility Model (GLEAMviz) (van den Broeck et al., 2011), has been used to assess the international spreading risk associated with the 2014 EVD outbreak, taking into account several realistic factors that influence the spreading (Gomes et al., 2014; Poletto et al., 2014). A detailed agent-based model, accounting for the spatial distribution of households and hospitals, geographic, and demographic information, and mobility patterns of individuals, has been presented in Merler et al. (2015) to assess the effectiveness of non-pharmaceutical intervention in Liberia. Agent-based models are very refined, but they provide valuable information only in extensive simulation campaigns with a deep knowledge of human behavior, and they are not amenable to analytical treatment.

The typical time scales of the progress of infectious diseases and the present lifestyle, with fast and frequent national and international travels, suggest that homogeneous mixing should be overcome in favor of approaches that explicitly account for the concurrent evolution of the dynamics of infectious diseases and formation of the network of contacts. Activity driven networks (ADNs) have been recently introduced to describe contact processes that evolve over time-varying networks (Perra et al., 2012), when timing and duration of connections happen over short time scales (Morris and Kretzschmar, 1997; Moody, 2002; Ghoshal and Holme, 2006; Butts, 2009; Holme and Saramäki, 2012), comparable with the dynamics of the process running on the network nodes. This modeling paradigm contrasts that of traditional connectivity-driven networks, where links between nodes have a long life span (Centola et al., 2007; Volz and Meyers, 2008; Schwartz and Shaw, 2010; Shaw and Schwartz, 2010; Jolad et al., 2012), resulting in the separation between the time scales of the dynamics of the network connections and the process evolution.

ADNs have been successfully used to study disease spreading in susceptible–infected–susceptible (SIS) and susceptible–infected–removed (SIR) models (Liu et al., 2014). Through a heterogeneous mean-field approach (Perra et al., 2012; Liu et al., 2014), spreading and immunization thresholds have been computed. These thresholds have been found to be considerably different from those computed on static networks, highlighting the need for more in-depth studies of epidemics on time-varying networks. ADNs can thus afford the possibility of formulating mathematically tractable, yet accurate, models of epidemic spreading, which overcome key limitations of mean-field compartmental and agent-based models. However, research on ADNs is in its infancy, and many efforts are currently under way to advance this field of investigation (Medus and Dorso, 2014; Rizzo et al., 2014; Sousa da Mata and Pastor-Satorras, 2015; Starnini and Pastor-Satorras, 2014; Sun et al., 2014). Toward a more realistic treatment of human factors, in Rizzo et al. (2014), we have studied the effect of individual behavior on the spreading of the epidemic in an SIS process. In particular, we have considered reduced activity of infected individuals, due to quarantine or to their debilitating health status, and self-protective behavior of healthy individuals on the basis of their risk perception. In Sun et al. (2014), the effect of memory phenomena on the epidemic threshold of SIS and SIR processes has been studied. These efforts have focused on hypothetical epidemic processes, and the validation of ADN models against real epidemic data is currently untapped.

In this paper, we formulate an ADN-based mathematical model of the 2014–2015 EVD outbreak in Liberia. The motivation for the selection of ADNs to model EVD is twofold. First, the incubation time of EVD, with a minimum of 2 and a maximum of 21 days (World Health Organization, 2014b), is compatible with the time scale of individual mobility patterns (González et al., 2008; Poletto et al., 2013). This implies that time-scale separation assumptions may yield incorrect predictions on the spread of the epidemic (Merler et al., 2015). Second, ADNs can be adapted to account for realistic phenomena that may be critical to the assessment of the severity and

duration of an EVD outbreak. Here, we have considered non-ideal and time-varying intervention policies (Merler et al., 2015), as well as reduced activity of infected individuals due to their debilitating health conditions (Rizzo et al., 2014). The proposed model considers several realistic forms of contagion, typical of EVD dynamics (Legrand et al., 2007; Althaus, 2014; Fisman et al., 2014; Gomes et al., 2014; Meltzer et al., 2014; Nishiura and Chowell, 2014; Rivers et al., 2014; Towers et al., 2014; Merler et al., 2015; Webb et al., 2015), and relies on a very detailed time-varying parameter set that accurately describes the epidemic state transitions. The epidemic model used in this work is based on the seminal Legrand's model for EVD spreading (Legrand et al., 2007), on which most of the recent research body on EVD rests (Fasina et al., 2014; Gomes et al., 2014; Lewnard et al., 2014; Meltzer et al., 2014; Pandey et al., 2014; Poletto et al., 2014; Rivers et al., 2014; Webb et al., 2015).

Legrand's model is a variant of the Susceptible–Exposed–Infected–Recovered (SEIR) model, which accounts for additional states to describe the specific dynamics of EVD. These additional states include hospitalized individuals and individuals who are dead but unsafely buried. SEIR models have been previously proposed for the study of EVD spreading (Althaus, 2014; CDC Stacks, 2014; Chowell et al., 2004; Fasina et al., 2014; Kiskowski, 2014) and efficiently forecasting the epidemic curve of the case count. Compared to Legrand's model, the SEIR model requires a reduced number of parameters to identify and is thus less prone to overfitting and overparametrization. However, Legrand's model is more effective in accurately resolving the evolution of the spreading, especially when the effect of hypothetical intervention and resource allocation policies should be assessed before their actual implementation (Fasina et al., 2014; Gomes et al., 2014; Lewnard et al., 2014; Pandey et al., 2014; Poletto et al., 2014; Rivers et al., 2014; Webb et al., 2015). Due to its tendency to overfitting, particular care must be taken in setting parameters for Legrand's model. Thus, most of the studies on Legrand's model do not attempt to identify the whole parameter set from the epidemic curve alone. Instead, they seek to establish as many parameters as possible from data collected in the field (such as the transition rate from infection to hospitalization and the percentage of infected that are hospitalized), and then identify the remainder of the parameters through optimization techniques (Fasina et al., 2014; Gomes et al., 2014; Lewnard et al., 2014; Meltzer et al., 2014; Poletto et al., 2014; Rivers et al., 2014; Webb et al., 2015). Here, we adopt Legrand's model to assess the effect of different intervention policies. In line with previous works, model parameters have been in part hypothesized from the existing literature (Khan et al., 1999; Legrand et al., 2007; Gomes et al., 2014; Rivers et al., 2014; The WHO Ebola Response Team, 2014; World Health Organization, 2014a; Merler et al., 2015), and in part identified through a least-square technique on the available dataset of the case count provided by the World Health Organization (WHO) (Centers for Disease Control and Prevention, 2014a; Rivers, 2014; World Health Organization, 2014a).

The remainder of the paper is organized as follows: in Section 2, we present an overview of network-based epidemic models and define some formalisms on graph theory and network-based epidemic models; in Section 3, we illustrate the proposed ADN-based model; in Section 4, we describe the model calibration and validation, and we present an implementation of the model to estimate the efficacy of timely intervention policies. Finally, we draw our conclusions in Section 5.

2. Epidemic models on networks

Time-varying networks are a powerful tool to study epidemic processes within populations and overcome the limitations of mean-field and static network-based models in modeling the inherent time-varying nature of human contacts (Frasca et al., 2006; Balcan and Colizza, 2009; Valdano et al., 2015). An epidemic model over a time-varying network is represented through a time-varying graph (Holme and Saramäki, 2012). A time-varying graph $\mathcal{G}$ consists of a pair of sets $\mathcal{G}=(\mathcal{N},\mathcal{E}(t))$. $\mathcal{N}$ is the *node set*, indexed by $i=1,\ldots,N$, where N is the cardinality of $\mathcal{N}$. $\mathcal{E}(t)\subseteq\mathcal{N}\times\mathcal{N}$ is the *link* (*or edge*) *set*, encapsulating the connections between nodes at a given time instant t. If two nodes $i,j\in\mathcal{N}\times\mathcal{N}$ are connected at time t, then $(i,j)\in\mathcal{E}(t)$. In epidemic models, links represent *contacts*, which constitute potential channels for the propagation of the infection: if $(i,j)\in\mathcal{E}(t)$, then node i may infect node j at time t, or vice versa. Thus, graph $\mathcal{G}=(\mathcal{N},\mathcal{E}(t))$ is often referred to as the *contact network* of the epidemic process. The set $\mathcal{N}_i(t)$ is the *neighborhood* of node i, containing all the nodes that are connected to it at time t, namely, $\mathcal{N}_i(t)=\{j\in\mathcal{N}\,|\,(i,j)\in\mathcal{E}(t)\}$.

The spread of an epidemic over a population is determined by the interplay of two dynamical processes: the spreading dynamics (how the epidemic spreads and evolve within the population) and the contact dynamics (how individuals get in contact to each other, creating the opportunity for the existence of infection channels). The former dynamics is usually defined by features that are inherent to the specific epidemic process, whereas the latter is determined by the mobility and activity patterns of the individuals. In general, the two dynamics are mutually coupled. For example, the probability to contract an infection may change with the travel activity of an individual (Ruan et al., 2006; Balcan and Colizza, 2009; Ni and Weng, 2009; Bajardi et al., 2011; Wang et al., 2012; Apolloni et al., 2013; Apolloni et al., 2014; Poletto et al., 2014) and, on the other hand, the state of health of an individual or his/her awareness about the risk of infection may affect his/her ability to travel or establish contacts with others (Poletti et al., 2009; Funk et al., 2009, 2010; Perra et al., 2011; House, 2011; Fenichel, 2011; Manfredi and D'Onofrio, 2013; Rizzo et al., 2014).

More formally, in a network-based epidemic model each individual is associated with a network node and labeled with $i=1,\ldots N$. The state of individual i is defined as $s_i(t)\in\mathcal{S}$, where $\mathcal{S}$ is a discrete set of states associated to the spreading dynamics. For example, $\mathcal{S}=\{S,I\}$ in a susceptible–infected–susceptible (SIS) epidemic model (Keeling and Rohani, 2011). The spreading dynamics of individual i over a time step Δt is formalized as

$$s_i(t+\Delta t)=f(s_i(t),\mathcal{S}_i(t),\mathcal{U}_s(t),t), \tag{1}$$

where $\mathcal{S}_i(t)=\{s_j(t),j\in\mathcal{N}_i(t)\}$ is the collection of states of individuals neighboring i, $\mathcal{U}_s(t)$ is a set of exogenous inputs (including exogenous causes of infection and drug administration), and $f(\cdot)$ is a deterministic or stochastic update function. The contact dynamics determines the evolution of the network of contacts in time and its evolution over a time step Δt is formalized as

$$\mathcal{E}(t+\Delta t)=g(\mathcal{E}(t),\mathcal{S}_N(t),\mathcal{U}_e(t),t), \tag{2}$$

where $\mathcal{S}_N(t)=\bigcup_{i=1}^{N}s_i(t)$ is the collection of all the individual states at time t, $\mathcal{U}_e(t)$ is a set of exogenous causes that may modify the dynamics of the network of contacts (travel bans, quarantine, *etc.*), and $g(\cdot)$ is a deterministic or stochastic update function.

Considerable work has been devoted to characterize the epidemic spreading assuming time-scale separation between the spreading and the contact dynamics, that is, hypothesizing that one dynamics evolve on a time-scale that is much faster than the other, yielding two limiting regimes, quenched and annealed (Pastor-Satorras and Vespignani, 2001; Newman, 2002; Yang Wang et al., 2003; Barrat et al., 2008; Castellano and Pastor-Satorras, 2010; Gómez et al., 2010; Goltsev et al., 2012; Boguñá et al., 2013). The former approach relies on the assumption that the contact dynamics evolves over a time-scale that is much slower than the spreading one; thus, the network of contacts $\mathcal{G}$ quenches in a static connectivity pattern that is approximated as a time-invariant network $\overline{\mathcal{G}}=(\mathcal{N},\overline{\mathcal{E}})$. In this case, the properties of the epidemic spreading can be related to the topological properties of the time-invariant graph, such as its adjacency matrix

(Yang Wang et al., 2003; Gómez et al., 2010). On the other hand, the annealed approximation posits that the contact dynamics is much faster than the spreading one. In this case, the epidemic spreading can be characterized on the basis of the averaged properties of the time-varying contact network (Pastor-Satorras and Vespignani, 2001; Newman, 2002).

Even though the analysis of the two limiting regimes has shed light on the dynamics of diffusion processes on networks, the availability of large time-resolved databases and efficient data-analysis techniques has revealed that such processes are mostly driven by the interplay of the spreading and the connection dynamics, which evolve at comparable time-scales (Vespignani et al., 2011; Perra et al., 2012; Valdano et al., 2015). Several studies have shown that the explicit treatment of the network topology, either time-invariant or time-varying, can substantially affect the epidemics (Barrat et al., 2008; Fibich and Gibori, 2010; Liu et al., 2014; Rizzo et al., 2014; Scholtes et al., 2014; Pastor-Satorras et al., 2015; Valdano et al., 2015; Rizzo and Porfiri, 2016). In this regard, ADNs are a promising paradigm to model such an intertwined dynamics (Perra et al., 2012; Liu et al., 2014; Rizzo et al., 2014; Sun et al., 2014; Rizzo and Porfiri, 2016).

The main difference between an agent-based epidemic model and an activity-driven model is that, while the former triggers connections through a metric criterion (two agents are connected if their Euclidean distance is less than a given threshold), in an activity driven model, connections are activated on the basis of an activity potential. The activity potential is described through a random variable that is hypothesized from the analysis of the motion patterns of individuals. Recent findings suggest that social interactions follow heavy-tailed or skewed statistical distributions (Holme, 2005; Onnela et al., 2007; Cattuto et al., 2010; Tang et al., 2010), and that mobility patterns are described by distributions of the same kind (González et al., 2008; Rhee et al., 2011). In the ADN formalism, the spatial dynamics is encapsulated in the activation mechanism, resorting to a single dynamical process, which accounts for both spreading and connection dynamics with the same time scale. This formalism has opened new paths in the theoretical analysis of realistic epidemic models (Liu et al., 2014; Rizzo et al., 2014), enabling us to complement approaches based on Monte Carlo simulation with new, rigorous results (van den Broeck et al., 2011; Camacho et al., 2014, 2015; Chowell and Nishiura, 2014; Lewnard et al., 2014). The following section illustrates in detail the proposed ADN-based model for EVD.

3. ADN model of EVD

In ADNs, links between individuals are established and removed at each time instant. The network assembly is based on an activity potential, which is the probability per unit time that a node will establish contacts with other nodes in the network (Perra et al., 2012; Liu et al., 2014; Rizzo et al., 2014). Each node has an activity potential x_i. Activity potentials do not change in time and are independent and identically distributed realizations of a random variable x, with a probability density function $F(x)$. The selection of $F(x)$ is a crucial step in the implementation of ADNs, since it determines the interactions within the network. In Perra et al. (2012), an analysis of three large, time-resolved datasets of contacts in social networks suggests a heavy-tail density function of the form $F(x) \propto x^{-\gamma}$, with $2 \leq \gamma \leq 3$. A typical distribution of the activity potential in an ADN is illustrated in Fig. 1, for a network with $N = 10^6$ nodes and $\gamma = 2.1$.

In its original incarnation (Perra et al., 2012), an activity firing rate $a_i = \eta x_i$ is assigned to each individual, where η is a constant scaling factor that regulates the average number of active nodes in the network in a unit time. In Rizzo et al. (2014), we have extended

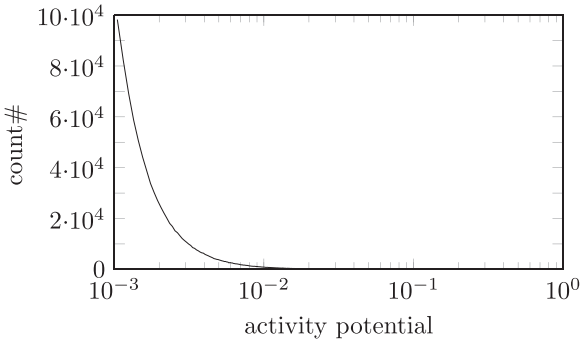

Fig. 1. Distribution of the activity potential x in an ADN of $N = 10^6$ nodes and $\gamma = 2.1$. Realizations x_i of the random variable x are constrained as $10^{-3} \leq x_i \leq 1$ to avoid the singularity close to zero.

the ADN modeling technique to account for time-varying changes in individual activity, such as those imposed by health status or behavior based on risk perception. For each individual, we have selected a time-varying scaling factor, whereby at each time instant the activity firing rate of agent i is $a_i(t) = \eta_i(t)x_i$.

The evolution of an ADN-based epidemic model in a time increment Δt, starting from a disconnected network of N nodes, is dictated by the following rules:

1. Node i, with $i = 1, \ldots, N$ becomes active with probability $a_i \Delta t$. If the node is active, it contacts m other nodes drawn at random from a uniform distribution, creating edges. If it is not active, no connections are created. At the end of this step, a graph is assembled;
2. The algorithmic rules of the considered epidemic model are run on the obtained graph, where contact and contagion may occur only between nodes that have been connected in the previous step; and
3. At the next time step $t + \Delta t$, all the edges in the network are removed and the process resumes.

Fig. 2 illustrates the evolution in a time step of duration Δt of a SIS model on an ADN with $N = 5$ nodes and $m = 2$ links per active node.

At each time instant, an ADN typically consists of a disconnected network composed of a number of star-like subnetworks, whose hubs are the nodes that are active during the time increment Δt. Active nodes have instantaneous degree larger than or equal to m, whereas non-active nodes usually have a smaller degree. Nodes with a larger activity potential are more likely to be activated at a given time. On the other hand, the integrated network constructed from the union of the instantaneous instances of the ADN will generally not be disconnected for t sufficiently large. It is such a network that ultimately controls the possibility of spreading the disease between the individuals.

Fig. 3 illustrates the evolution of an integrated ADN network of $N = 500$ nodes, a common value of the scaling parameter $\eta = 4.5$, a number of links per active node $m = 5$, and the exponent of the activity distribution $\gamma = 2.1$. In Fig. 3, snapshots of the integrated network are illustrated at time instants $t = 0, \Delta t, 2\Delta t$, and $3\Delta t$, and larger nodes are associated with higher values of the activity potential. Consistently with the choice of a power law for $F(x)$, we observe that only a small fraction of the nodes have a high activity potential, whereas the majority has a rather small activity potential. Nodes with high activity potential will be those creating more contacts over time, acting as hubs in the integrated network. Due to their high contact rate, such nodes are fundamental for the epidemic spreading, regardless of their health status. If they are infected, they will have a high probability to contact and infect healthy individuals. On the other hand, if they are healthy, they

will have a high probability to contact infected individuals and be infected.

We adopt the state transitions from Legrand's model (Legrand et al., 2007), which is a variant of the Susceptible–Exposed–Infected–Removed (SEIR) model (Brauer and Castillo-Chavez, 2011), including two states related to hospitalization (H) and death followed by a traditional funeral, without immediate safe burial (F).

The removed state (R) indicates individuals that cannot contribute any more to the dynamics of the epidemic spreading. This state contains individuals who have recovered and are immune, and those who have died and have been safely buried. In our EVD model, we partition the removed state into two states: recovered (R_R); and dead and safely buried (R_D). The dynamics of the state transitions is schematized in Fig. 4. Similar to Rizzo et al. (2014), we assume that people infected with EVD and not hospitalized have a lower probability to come in contact with other individuals, as they will move less due to their debilitated health. Yet, such probability is non-zero, as they may infect those who take care of them, that is, friends, parents, and relatives. Thus, we differentiate the activity of susceptible and exposed individuals from that of infected ones, using two different activity rates, namely, η_{SE} and η_I.

Model parameters belong to three categories: probabilities of infection, transition rates, and transition fractions. Probabilities of infection are indicated with $\lambda_\bullet$, where the subscript identifies (I), (H), or (F) states. These parameters indicate the per-contact probability of a susceptible individual to contract the epidemic by contacting an infected (I), hospitalized (H), or a dead and not safely buried (F) individual. Transition rates are indicated with $\mu_{\bullet\times}$, where subscripts indicate any two different states of the epidemic model. The inverse of a transition rate $1/\mu_{\bullet\times}$ quantifies the average time for an individual to transition from state $\bullet$ to state $\times$. Similarly, a transition fraction is denoted with $\delta_{\bullet\times}$ and quantifies the fraction of individuals in state $\bullet$ that transition to state $\times$. Table 1 summarizes the parameters of the model.

The EVD model rules, dictating the state transitions in our ADN-based model, are as follows:

1. If a susceptible (S) individual is in contact with an infected (I), hospitalized (H), or dead and not safely buried (F) individual, he/she will contract the infection and transition to the exposed (E) state with per-contact and per unit time transmission probability λ_I, λ_H, and λ_F, respectively;
2. An exposed individual (E) transitions to the infected and symptomatic (I) state with rate μ_I;
3. An infected and symptomatic individual (I) transitions to one of the three states: hospitalized (H), dead and not safely buried (F), recovered (R_R), and dead and safely buried (R_D). A fraction δ_{IH} of infected individuals is hospitalized with rate μ_{IH}; a fraction δ_{IF} remains in the community, eventually dies, and receives traditional funeral rituals, without safe burial, with rate μ_{IF}; a fraction δ_{IR_R} recovers with rate μ_{IR_R}; and a fraction δ_{IR_D} dies in the community and is safely buried by a burial team with a rate μ_{IR_D}. The constraint $\delta_{IH}+\delta_{IF}+\delta_{IR_R}+\delta_{IR_D}=1$ holds;
4. A hospitalized individual (H) transitions to the recovered (R_R) or the dead and safely buried (R_D) state. A fraction δ_{HR_R} will recover with rate μ_{HR_R}, whereas a fraction δ_{HR_D} will die with rate

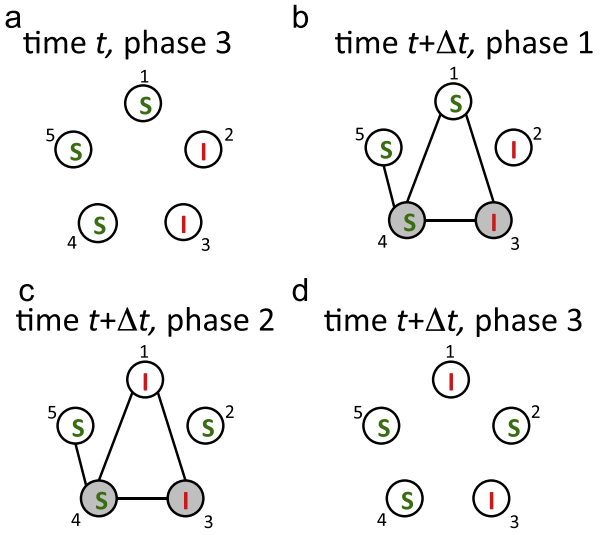

Fig. 2. An SIS epidemic model evolving on an ADN with $N=5$ nodes and $m=2$ links per active node. Nodes' health states are encircled, and active nodes are shaded. (a) At the last phase of time t, the ADN is disconnected and nodes 2 and 3 are infected. Between t and $t+\Delta t$: (b) nodes 3 and 4 become active and contact nodes 4 and 1, and 5 and 1, respectively; (c) the epidemic process evolves, so that node 3 infects node 1, nodes 2, 4, and 5 remain in the susceptible state, and node 2 recovers; and (d) time Δt has elapsed and all the network edges are removed before a new time increment is initiated.

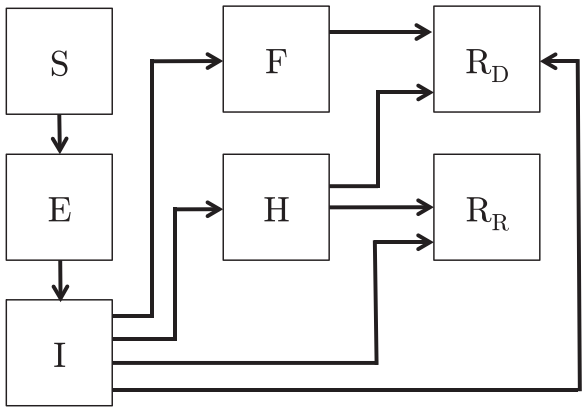

Fig. 4. State transitions in a seven-state EVD model. The states are S, susceptible; E, exposed (infected, non-symptomatic); I, infected (symptomatic); H, hospitalized; F, dead but not buried; R_R, recovered; and R_D, dead and safely buried.

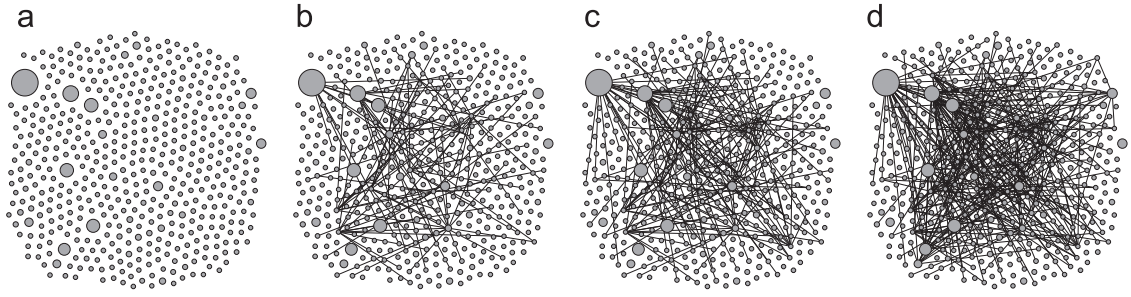

Fig. 3. Evolution of an integrated ADN of $N=500$ nodes, $\gamma=2.1$, $\eta=4.5$, $m=10$. Realizations x_i of the random variable x are constrained as $10^{-3}\le x_i\le 1$ to avoid the singularity close to zero. Larger nodes are associated with higher values of the activity potential x_i. Snapshots are taken at (a) $t=0$, (b) $t=\Delta t$, (c) $t=2\Delta t$, and (d) $t=3\Delta t$.

Table 1
Parameters of the activity driven EVD model.

Parameter	Meaning
η_{SE}, η_I	Activity rate
λ_I, λ_H, λ_F	Probability of infection
μ_{EI}, μ_{IH}, μ_{IF}, μ_{IR_R}, μ_{IR_D}, μ_{HR_R}, μ_{HR_D}, μ_{FR_D}	Transition rate
δ_{IH}, δ_{IF}, δ_{IR_R}, δ_{IR_D}, δ_{HR_R}, δ_{HR_D}	Transition fraction

μ_{HR_D} and then is safely buried. The constraint $\delta_{HR_R}+\delta_{HR_D}=1$ holds; and

5. Dead people who have not been handled by a burial team will remain infectious until burial. Individuals in the dead and not safely buried (F) state will be buried with a rate μ_{FR_D} and transition to the dead and buried (R_D) state.

4. Results

4.1. Model calibration

The model has been calibrated on the basis of available WHO epidemic data (Centers for Disease Control and Prevention, 2014a; Rivers, 2014; World Health Organization, 2014a). The calibration of highly detailed epidemic models, like the one presented in this paper, offers two main challenges. First, the large number of parameters to identify may lead to overfitting (VirginiaTech Network Dynamics & Simulation Science and Laboratory, 2014), whereby different combinations of parameter can yield similar epidemic curves. This requires parameter identification to be supervised by field experts, who should inform the algorithms with realistic initial guesses for the parameter set to be identified and support the selection of a particular parameter set among several candidates. Second, data are only available in aggregated form. Refined information, such as non-aggregated case counts, noise-free data sampled at a constant rate, or global databases of the network of contacts are not accessible. While the need for detailed and reliable data has been frequently put forward by the scientific community (Merler et al., 2015), the current state-of-the-art offers compelling evidence for advancing mathematically tractable, epidemic models with few parameters that can be identified from available data.

Our EVD model is calibrated on the WHO count of confirmed EVD cases in Liberia, from April 8, 2014 to December 31, 2014, yielding a time span of 268 days (Centers for Disease Control and Prevention, 2014a; Rivers, 2014; World Health Organization, 2014a). The dynamics of EVD spreading is different in each affected country and even in different districts of the same country, thus, the identification of the parameter set depends on the geographic area under observation (Lewnard et al., 2014; Rivers et al., 2014; Camacho et al., 2015). In order to mitigate the risk for overfitting because of overparametrization, grounded on previous modeling efforts (Legrand et al., 2007; Althaus, 2014; Fisman et al., 2014; Gomes et al., 2014; Meltzer et al., 2014; Nishiura and Chowell, 2014; Rivers et al., 2014; Towers et al., 2014; Merler et al., 2015; Webb et al., 2015) and on the study of the WHO situation reports (World Health Organization, 2014a), we set epidemic-specific parameters from the available literature and field reports, and identify only those related to the network activity, which are strictly pertinent to our modeling strategy. Hence, model parameters are determined in three different ways.

Parameters in Table 2 are independent of the application of intervention measures. Thus, they are treated as constant in time and are obtained from the technical literature (Rivers et al., 2014; World Health Organization, 2014a; Merler et al., 2015). Parameters

Table 2
Time-invariant parameters of the activity driven EVD model.

Parameter	Value
λ_I	0.16
λ_F	0.49
μ_{EI}	0.09 days^{-1}
μ_{IF}	0.13 days^{-1}
μ_{IR_R}	0.13 days^{-1}
μ_{IR_D}	0.13 days^{-1}
μ_{HR_R}	0.22 days^{-1}
μ_{HR_D}	0.24 days^{-1}
μ_{FR_D}	0.5 days^{-1}
δ_{IR_R}	0
δ_{HR_R}	0.46
δ_{HR_D}	0.54

Table 3
Time-varying parameters of the activity driven EVD model. Phase 1: before mid-August 2014 (day 0 to 130); Phase 2: between mid-August and mid-October 2014 (day 131 to 190); and Phase3: after mid-October 2014 (from day 191 onward).

Parameter	Phase 1	Phase 2	Phase 3
λ_H	0.33	0.02	0.02
μ_{IH}	0.1 days^{-1}	0.2 days^{-1}	0.43 days^{-1}
δ_{IH}	0.51	0.80	0.89
δ_{IF}	0.1	0.05	0.01
δ_{IR_D}	0.39	0.15	0.10

in Table 3, on the other hand, depend on the level of intervention in the field, which we know has increased from mid-August 2014 (Merler et al., 2015). Actions in the field have included: (i) an increase in the number of hospital beds for EVD patients; (ii) the exclusive admission of patients in symptomatic states to Ebola treatment units, with a consequent reduction of the probability of infection; (iii) an increase in the number of safe burial procedures; and (iv) improvements in the implementation of contact tracing procedures (Merler et al., 2015).

To model this growing level of intervention, we hypothesize that parameters in Table 3 are time-varying. In an effort to minimize the complexity of such a time variation, we let such parameters take different values with step-like changes, during three phases: before mid-August (day 0 to 120), between mid-August and mid-October (day 121 to 190), and after mid-October (day 181 onward). The parameters for the first two phases are selected from the available literature (Rivers et al., 2014; World Health Organization, 2014a; Merler et al., 2015), while those in the third phase reflect the further increase in the efficiency of the intervention level, which we know has occurred in many districts of Liberia, especially in Montserrado (the Capital County), where a strong improvement in hospitalization, laboratory testing and body collection in October has been reported by the CDC (Nyenswah et al., 2014). Although the parameter set for the third phase has not been confirmed in the literature, our selection reflects the application of an almost ideal intervention in the field confirmed by recent WHO statements (World Health Organization, 2015). To prevent overfitting, we have verified that small variations of values of the selected parameters do not significantly affect the predictive performance of the model, leading to a satisfactory agreement with the epidemic data.

The remaining ADN-related parameters, that is, the number of contacts per unit time of active nodes, m, the scaling factor of the activity of susceptible and exposed individuals, η_{SE}, and that of infected and symptomatic individuals, η_I, have been identified as follows. The epidemic curve of cumulative WHO-confirmed EVD

cases in Liberia (Centers for Disease Control and Prevention, 2014a) from April 8, 2014 to December 31, 2014 (268 days) has been resampled using a zero-order-hold (that is, the number of cases has been kept constant in those days where no increments occurred) to obtain an epidemic curve $I_{\mathrm{WHO}}(t)$ in discrete time, with constant sampling time $\Delta t = 1$ day and $t = 0 \ldots 267$. Then, different instances of the ADN model are run on a network with $N = 4.6 \cdot 10^6$ nodes (about the same size of Liberia population) and with $\Delta t = 1$ day, varying the parameters m, η_{SE}, and η_I, respectively, over a three-dimensional parameter grid with $8 \times 7 \times 9 = 504$ points. We varied the parameters in the following ranges: $m \in \{3, \ldots, 10\}$ with step 1, $\eta_{SE} \in \{3.0, \ldots, 6.0\}$ with step 0.5, and $\eta_I \in \{2.0, \ldots, 6.0\}$ with step 0.5. The initial number of infected individuals in the model runs has been set equal to the number of cases at the beginning of the observation window, that is, $I_{\mathrm{WHO}}(0) = 21$. Each instance of the model has been run for 50 independent trials, randomizing the location in the network of the individuals initially infected, and the obtained epidemic curves have been averaged over the 50 trials, obtaining a simulated epidemic curve $I_S(m, \eta_{SE}, \eta_I, t)$ for each point of the parameter grid, that is, for each combination of values of the three parameters. Parameters have been identified according to a mean-square error criterion, where the triplet m, η_{SE}, and η_I minimizes

$$J(m, \eta_{SE}, \eta_I) = \frac{1}{268} \sum_{t=0}^{267} \left(I_{\mathrm{WHO}}(t) - I_S(m, \eta_{SE}, \eta_I, t) \right)^2. \quad (3)$$

The identified parameter values are $m = 7$, $\eta_{SE} = 4.5$, and $\eta_I = 3.2$. These parameters were then used to validate the model on a further portion of the epidemic curve, $I_{\mathrm{WHO}}(t)$, related to confirmed cases from January 1, 2015, to December 2, 2015.

Additional simulations have been performed to assess the role of the exponent of the activity distribution, γ, in the evolution of the epidemic. A good fit has been found setting $\gamma = 2.1$. This value is consistent with other findings in the literature, which posit that social interactions follow heavy-tailed or skewed statistical distributions (Holme, 2005; Onnela et al., 2007; Cattuto et al., 2010; Tang et al., 2010).

For clarity, a typical evolution of the EVD epidemic is illustrated in Fig. 5 for a smaller population than Liberia and parameters in Table 3 chosen from Phase 1. We show snapshots for three salient instants in the spreading dynamics. Fig. 5(a) depicts the initial instant, where a given number of infected individuals are present in an otherwise healthy population. The possibility of EVD to cause an epidemic outbreak depends on several factors, such as the number of infected individuals, their activity, and the probability of infection. Fig. 5(b) refers to the epidemic peak, which is the instant when EVD has infected the largest number of individuals. The epidemic peak is usually when the maximum of resources has to be employed to fight the outbreak. However, the occurrence of the peak is generally followed by the fading of the outbreak. Thus, the earlier the peak occurs, the earlier the outbreak will come to an end. Finally, Fig. 5(c) illustrates the end of the epidemic, when all the individuals are either in the susceptible or in the removed state (dead and safely buried or recovered). A return of the outbreak is impossible, unless new infected individuals join the population.

4.2. Model validation

To offer some validation for the model, we have kept the parameters to the values determined during the identification phase and we have run 50 instances of the model starting from the same initial value of 21 cases and randomizing their location in the network. Then, an epidemic curve averaged over the 50 trials has been obtained and compared with the available WHO-confirmed cumulative curve of EVD cases (Centers for Disease Control and Prevention, 2014a). Fig. 6 illustrates the simulated curve as a function of time, superimposed to available data. As expected, the model accurately replicates the case count for the first 268 days used for calibration, capturing the slow increase from day 0 to day 90 followed by the dramatic increase until day 190, and a more moderate increase from day 190 to day 268. Beyond these first 268 days, we report model predictions for other 337 days, until December 2, 2015, forecasting a rather modest increase of the case count. In April 2015, in fact, Liberia was going to be declared Ebola-free (LiveScience, 2015) until a new case was reported (BBC, 2015). At the moment of writing this paper, only a few additional cases have been reported in Liberia, suggesting that the epidemic is close to eradication.

4.3. Assessment of the effect of intervention policies

Our model can be effectively used to estimate the efficacy of timely intervention policies. To this aim, we contemplate the possibility of shifting the time when we have seen an increase in the level of field interventions (day 121 in Table 3) to an earlier day. In other words, we run our EVD model by only changing the time when the transition between Phase 1 and Phase 2 takes place. We consider the following possible dates: early July (day 76), early June (day 46), and early May (day 16). Fig. 7 displays the forecasted cumulative case that counts associated with the selected times. As expected, anticipating the implementation of more effective intervention policies drastically reduces the epidemic spreading. For example, the outbreak would have ended with a 72% reduction of the total Ebola cases (*i.e.*, 2830 rather than 9922) by anticipating the increase in the level of interventions to day 76.

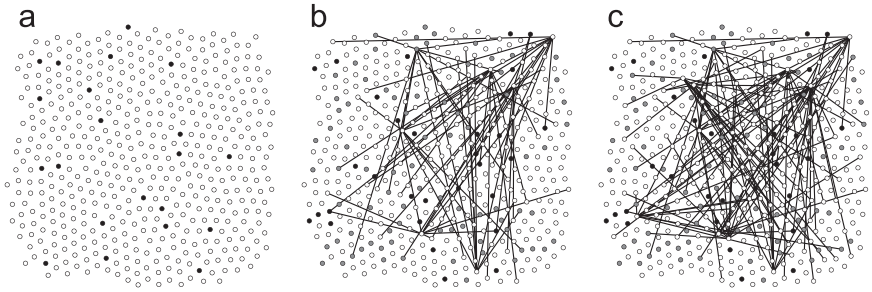

Fig. 5. Simulation snapshots of an EVD epidemic on an ADN with $N = 500$ nodes, evolving according to our model. The epidemic state of each node is coded in gray scale and the links between nodes identify contacts. (a) Initial state ($t = 0$ days): 21 infected and symptomatic individuals are in the population (black nodes) and the remaining 479 individuals are susceptible (white nodes). (b) Epidemic peak ($t = 53$ days): 7 individuals are infected and symptomatic (black nodes), 39 individuals are hospitalized and 14 individuals are dead but not safely buried (both represented with gray nodes), and the remaining 440 individuals are susceptible. (c) Outbreak end ($t = 130$ days): 30 individuals are dead and are safely buried (black nodes), 82 individuals have recovered (gray nodes), and the remaining 388 individuals are still susceptible (white nodes).

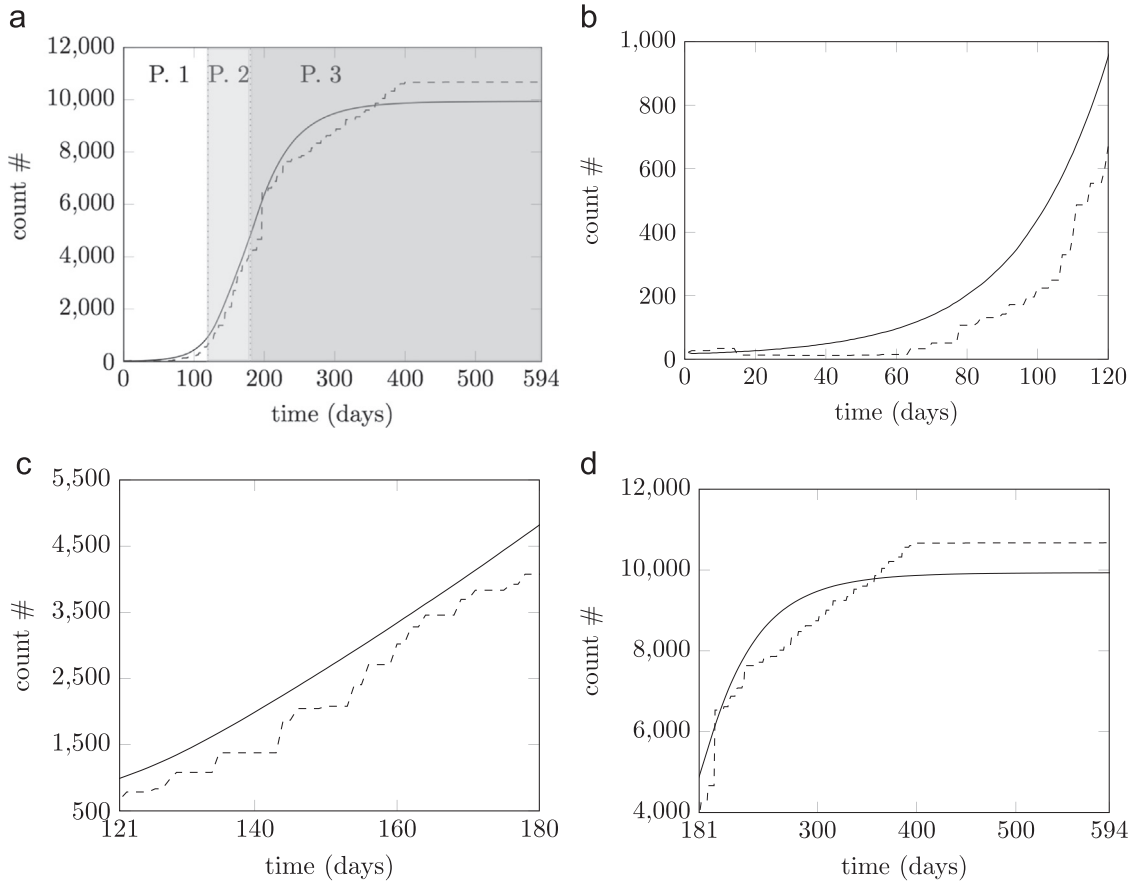

Fig. 6. Calibration of the model on real data and model predictions. In (a), the comparison between model predictions and field data involves the entire duration of the spreading from 4/8/2014 to 12/2/2015. The solid line shows model results in terms of the cumulative number of cases, and the dashed line shows the cumulative case count reported by WHO and CDC in Liberia (Centers for Disease Control and Prevention, 2014a). Shaded regions identify the three phases of the intervention policy hypothesized in Table 3. The step-like discontinuity in the case count around sample 200 is likely due to data corruption. This observation is supported by the corresponding death count, which decreases correspondingly (while it should always increase) (Centers for Disease Control and Prevention, 2015). In (b)–(d), the three phases of the intervention policies are separately illustrated. Model predictions are illustrated in (d), from day 268 onwards.

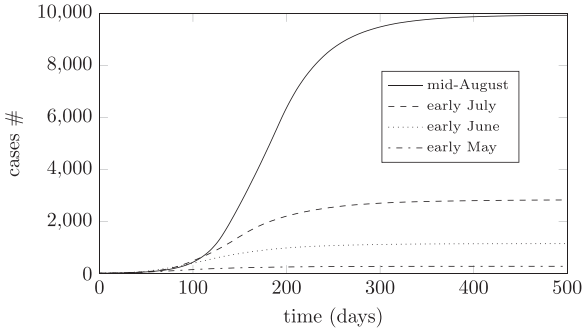

Fig. 7. Prediction of the cumulative number of cases in Liberia between 4/8/2014 and 8/20/2015, by varying the time of the transition between Phase 1 and Phase 2, defining when the level of interventions is increased. The dates of such transitions are detailed in the legend. Simulations are averaged over 50 independent trials.

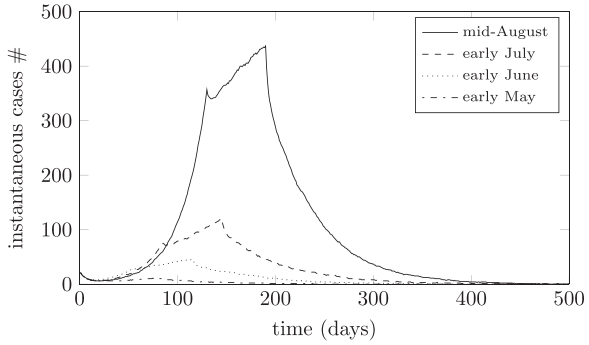

Fig. 8. Prediction of the instantaneous number of cases in Liberia between 4/8/2014 and 8/20/2015, by varying the time of the transition between Phase 1 and Phase 2, defining when the level of interventions is increased. The dates of such transitions are detailed in the legend. Simulations are averaged over 50 independent trials.

The beneficial effect of an earlier implementation of superior intervention policies is also noted in the timing of the epidemic peak. Fig. 8 displays the trend of the instantaneous number of infected individuals for the same instances considered in Fig. 7. We observe that the occurrence of the peak recedes when these superior intervention policies are applied earlier. A timely implementation would thus also be beneficial to a faster resolution of the outbreak.

The model can also be used to estimate the needed infrastructure to face the outbreak, in the form of the number of beds available for EVD patients. Fig. 9 shows the number of hospitalized persons as a function of time for the same instances considered in Figs. 7 and 8. To implement a desired intervention policy at a given time, the number of available hospital beds must larger than the number of persons that should be theoretically hospitalized. Therefore, the peak value of the number of hospitalized persons predicted by the model can be used to estimate the numbers of beds that should be made available in the country. Fig. 9 suggests that anticipating the implementation of more effective intervention policies determines the infrastructure that should be

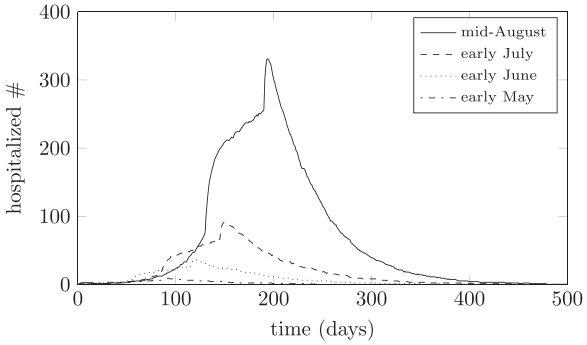

Fig. 9. Prediction of the instantaneous number of hospitalized patients in Liberia between 4/8/2014 and 8/20/2015, by varying the time of the transition between Phase 1 and Phase 2, defining when the level of interventions is increased. The dates of such transitions are detailed in the legend. Simulations are averaged over 50 independent trials.

available. While the mid-August timing is estimated to require 331 beds, anticipating it to early in July would have only required 91 beds.

5. Conclusions

EVD is a global challenge that is engaging doctors, scientists, and experts worldwide. In 2014–2015, we have experienced the most severe outbreak in West Africa, while the rest of the world has been threatened by the possibility of a global outbreak. Since neither qspecific pharmaceutical treatments nor vaccines were available, the only way to contrast the outbreak was by implementing non-pharmaceutical intervention policies. In this context, reliable mathematical models can provide qualitative and quantitative information to inform policy makers on the implementation of intervention policies and prophylactic strategies.

In this paper, we have proposed a novel model for EVD based on ADNs. The modeling technique offers an effective trade-off between mathematical tractability and computational complexity. This is especially important as we seek to rapidly-and-accurately assess the effectiveness of intervention policies based on a rather limited dataset of field data. To the best of our knowledge, this is the first effort to demonstrate the possibility of using ADNs to study real epidemics. ADN-based models do not explicitly reproduce the geographical movements of individual. Rather, they incorporate this information in the form of an activity potential, which quantifies the number of contacts an individual can generate in a time step.

We have specialized the model to the 2014–2015 EVD spreading in Liberia. The model has been calibrated on field data over the first 9 months of the infection and utilized to predict the evolution of the epidemic for the following 12 months, up to December 2, 2015. While the model depends on minimal numbers of parameters to be identified from available field data, it accounts for several behavioral and epidemiological factors that are likely to contribute to EVD spreading. For example, our model considers different activities for healthy and symptomatic individual, and interventions with a different intensity over time. Moreover, we have performed a what-if analysis on the effect of an earlier application of intervention policies that were actually implemented in August, 2014. Our results further stress the paramount importance of an early and prompt response to such threat and that an earlier application of the same intervention policies would have drastically mitigated the epidemic spreading, in terms of number of cases, duration of the outbreak, and required infrastructure. Despite the limited quantity and quality of data, the predictive capabilities of the proposed model are satisfactory, and will be refined in the future as new data become available.

Future work will seek to further refine the modeling framework to describe geographic locality of contacts and phenomena of link persistency and memory. Moreover, the network of contacts generated by the ADN model will be analyzed in the framework of time-varying networks to characterize the propensity of individuals to contract the infection, or to estimate the probability for an individual to be in the incubation state. This will aid in the implementation of intervention policies for individuals who are not symptomatic, yet have a stronger likelihood to transition to the symptomatic state and transmit the infection.

Acknowledgments

Alessandro Rizzo warmly thanks the Honors Center of Italian Universities (H2CU) for housing and scholarship support.

References

Ajelli, M., Gonçalves, B., Balcan, D., Colizza, V., Hu, H., Ramasco, J.J., Merler, S., Vespignani, A., 2010. Comparing large-scale computational approaches to epidemic modeling: agent-based versus structured metapopulation models. BMC Infect. Dis. 10, 190.

Althaus, C.L., 2014. Estimating the reproduction number of Ebola virus (EBOV) during the 2014 outbreak in West Africa. PLoS Curr. 6, 1–7.

Apolloni, A., Poletto, C., Colizza, V., 2013. Age-specific contacts and travel patterns in the spatial spread of 2009 H1N1 influenza pandemic. BMC Infect. Dis. 13, 176.

Apolloni, A., Poletto, C., Ramasco, J.J., Jensen, P., Colizza, V., 2014. Metapopulation epidemic models with heterogeneous mixing and travel behaviour. Theor. Biol. Med. Model. 11 (1), 3.

Bajardi, P., Poletto, C., Ramasco, J.J., Tizzoni, M., Colizza, V., Vespignani, A., 2011. Human mobility networks, travel restrictions, and the global spread of 2009 H1N1 pandemic. PLoS One 6 (1), e16591.

Balcan, D., Colizza, V., 2009. Multiscale mobility networks and the spatial spreading of infectious diseases. Proc. Natl. Acad. Sci. 106 (51), 21484–21489.

Barrat, A., Barthelemy, M., Vespignani, A., 2008. Dynamical Processes on Complex Networks. Cambridge University Press, Cambridge, UK.

BBC, 2015. Ebola case undermines Liberia disease-free hopes. ⟨http://www.bbc.com/news/world-africa-31991748⟩.

Boguñá, M., Castellano, C., Pastor-Satorras, R., 2013. Nature of the epidemic threshold for the susceptible–infected–susceptible dynamics in networks. Phys. Rev. Lett. 111, 068701.

Brauer, F., 2008. Epidemic models with heterogeneous mixing and treatment. Bull. Math. Biol. 70 (7), 1869–1885. http://dx.doi.org/10.1007/s11538-008-9326-1.

Brauer, F., Castillo-Chavez, C., 2011. Mathematical Models in Population Biology and Epidemiology. Springer, New York.

Butts, C.T., 2009. Revisiting the foundations of network analysis. Science 325 (5939), 414–416.

Camacho, A., Kucharski, A.J., Funk, S., Breman, J., Piot, P., Edmunds, W.J., 2014. Potential for large outbreaks of Ebola virus disease, Epidemics 9, 70–78.

Camacho, A., Kucharski, A., Aki-Sawyerr, Y., White, M.A., Flasche, S., Baguelin, M., Pollington, T., Carney, J.R., Glover, R., Smout, E., Tiffany, A., Edmunds, W.J., Funk, S., 2015. Temporal changes in Ebola transmission in Sierra Leone and implications for control requirements: a real-time modelling study. PLoS Curr. Outbreaks 7, 1–20.

Castellano, C., Pastor-Satorras, R., 2010. Thresholds for epidemic spreading in networks. Phys. Rev. Lett. 105, 218701.

Cattuto, C., Van den Broeck, W., Colizza, V., Pinton, J.-F., Vespignani, A., 2010. Dynamics of person-to-person interactions from distributed RFID sensor networks. PLoS One 5 (7), e11596.

CDC Stacks, 2014. Generic EbolaResponse (ER): Modeling the spread of disease impact & intervention, Version 2.5, ⟨http://stacks.cdc.gov/view/cdc/24900⟩.

Centers for Disease Control and Prevention, 2015. 2014 Ebola Outbreak in West Africa – Reported Cases Graphs, ⟨http://www.cdc.gov/vhf/ebola/outbreaks/2014-west-africa/cumulative-cases-graphs.html⟩.

Centers for Disease Control and Prevention, 2014a. Ebola Outbreak in West Africa – Case Counts, ⟨http://www.cdc.gov/vhf/ebola/outbreaks/2014-west-africa/case-counts.html⟩.

Centers for Disease Control and Prevention, 2014b. Cases of Ebola Diagnosed in the United States, ⟨http://www.cdc.gov/vhf/ebola/outbreaks/2014-west-africa/united-states-imported-case.html⟩.

Centers for Disease Control and Prevention, 2014c. Top 10 Ebola Response Planning Tips: Ebola Readiness Self-assessment for State and Local Public Health Officials, ⟨http://www.cdc.gov/vhf/ebola/outbreaks/prepared-ness/planning-tips-top10.html⟩.

Centola, D., González-Avella, J.C., Eguíluz, V.M., San Miguel, M., 2007. Homophily, cultural drift, and the co-evolution of cultural groups. J. Confl. Resolut. 51 (6), 905–929.
Choe, S., Lee, S., 2015. Modeling optimal treatment strategies in a heterogeneous mixing model. Theor. Biol. Med. Model. 12 (1), 28.
Chowell, G., Nishiura, H., 2014. Transmission dynamics and control of Ebola virus disease (EVD): a review. BMC Med. 12 (1), 196.
Chowell, G., Hengartner, N.W., Castillo-Chavez, C., Fenimore, P.W., Hyman, J.M., 2004. The basic reproductive number of Ebola and the effects of public health measures: the cases of Congo and Uganda. J. Theor. Biol. 229, 119–126.
Fasina, F.O., Shittu, A., Lazarus, D., Tomori, O., Simonsen, L., Viboud, C., Chowell, G., 2014. Transmission dynamics and control of Ebola virus disease outbreak in Nigeria, July to September 2014. Eurosurveillance 19 (40), 20920.
Fenichel, E.P., 2011. Adaptive human behavior in epidemiological models. Proc. Natl. Acad. Sci. U. S. A. 108 (15), 6306–6311.
Ferguson, N., 2007. Capturing human behaviour. Nature 446 (7137), 733.
Fibich, G., Gibori, R., 2010. Aggregate diffusion dynamics in agent-based models with a spatial structure. Oper. Res. 58 (5), 1450–1468.
Fisman, D., Khoo, E., Tuite, A., 2014. Early epidemic dynamics of the West African 2014 Ebola outbreak: estimates derived with a simple two-parameter model. PLoS Curr. 6, 1–13.
Frasca, M., Buscarino, A., Rizzo, A., Fortuna, L., Boccaletti, S., 2006. Dynamical network model of infective mobile agents. Phys. Rev. E 74 (3), 036110.
Funk, S., Gilad, E., Watkins, C., Jansen, V.A.A., 2009. The spread of awareness and its impact on epidemic outbreaks. Proc. Natl. Acad. Sci. 106 (16), 6872–6877.
Funk, S., Salathé, M., Jansen, V.A., 2010. Modelling the influence of human behaviour on the spread of infectious diseases: a review. J. R. Soc. Interface 7 (50), 1247–1256.
Ghoshal, G., Holme, P., 2006. Attractiveness and activity in internet communities. Physica A: Stat. Mech. Appl. 364, 603–609.
Goltsev, A.V., Dorogovtsev, S.N., Oliveira, J.G., Mendes, J.F.F., 2012. Localization and spreading of diseases in complex networks. Phys. Rev. Lett. 109, 128702.
Gomes, M.F.C., Pastore, A., Rossi, L., Chao, D., Longini, I., Halloran, M.E., Vespignani, A., 2014. Assessing the international spreading risk associated with the 2014 West African Ebola outbreak. PLoS Curr. 6, 1–20.
Gómez, S., Arenas, A., Borge-Holthoefer, J., Meloni, S., Moreno, Y., 2010. Discrete-time Markov chain approach to contact-based disease spreading in complex networks. Europhys. Lett. 89 (3), 38009.
González, M.C., Hidalgo, C.A., Barabási, A., 2008. Understanding individual human mobility patterns. Nature 453 (7196), 779–782.
Holme, P., 2005. Network reachability of real-world contact sequences. Phys. Rev. E 71, 046119.
Holme, P., Saramäki, J., 2012. Temporal networks. Phys. Rep. 519 (3), 97–125.
House, T., 2011. Modelling behavioural contagion. J. R. Soc. Interface/R. Soc. 8 (59), 909–912.
Jolad, S., Liu, W., Schmittmann, B., Zia, R.K.P., 2012. Epidemic spreading on preferred degree adaptive networks. PLoS One 7 (11), e48686.
Keeling, M.J., Eames, K.T.D., 2005. Networks and epidemic models. J. R. Soc. Interface 2 (4), 295–307.
Keeling, M.J., Rohani, P., 2011. Modeling Infectious Diseases in Humans and Animals. Princeton University Press, Princeton, NJ, USA.
Khan, A.S., Tshioko, F.K., Heymann, D.L., Le Guenno, B., Nabeth, P., Kerstiens, B., Fleerackers, Y., Kilmarx, P.H., Rodier, G.R., Nkuku, O., Rollin, P.E., Sanchez, A., Zaki, S.R., Swanepoel, R., Tomori, O., Nichol, S.T., Peters, C.J., Muyembe-Tamfum, J.J., Ksiazek, T.G., 1999. The reemergence of Ebola hemorrhagic fever, Democratic Republic of the Congo, 1995. J. Infect. Dis. 179 (Supplement 1), S76–S86.
Kiskowski, M.A., 2014. A three-scale network model for the early growth dynamics of 2014 West Africa Ebola epidemic. PLoS Curr. 6, 1–28.
Legrand, J., Grais, R.F., Boelle, P.Y., Valleron, A.J., Flahault, A., 2007. Understanding the dynamics of Ebola epidemics. Epidemiol. Infect. 135 (4), 610–621.
Lewnard, J.A., Ndeffo Mbah, M.L., Alfaro-Murillo, J.A., Altice, F.L., Bawo, L., Nyenswah, T.G., Galvani, A.P., 2014. Dynamics and control of Ebola virus transmission in Montserrado, Liberia: a mathematical modelling analysis. Lancet Infect. Dis. 14, 1189–1195.
Liu, S., Perra, N., Karsai, M., Vespignani, A., 2014. Controlling contagion processes in activity driven networks. Phys. Rev. Lett. 112, 118702.
LiveScience, 2015. Liberia, Guinea on Track to Contain Ebola, ⟨http://www.livescience.com/48962-ebola-transmission-rate-down.html⟩.
Manfredi, P., D'Onofrio, A. (Eds.), 2013. Modeling the Interplay Between Human Behavior and the Spread of Infectious Diseases. Springer-Verlag, New York, NY, USA.
Medus, A.D., Dorso, C.O., 2014. Memory effects induce structure in social networks with activity-driven agents. J. Stat. Mech.: Theory Exp. 2014 (9), P09009.
Meltzer, M.I., Atkins, C.Y., Santibanez, S., Knust, B., Petersen, B.W., Ervin, E.D., Nichol, S.T., Damin, I.K., Washington, M.L., 2014. Estimating the future number of cases in the Ebola epidemic—Liberia and Sierra Leone, 2014–2015. Morb. Mortal. Wkly. Rep. Suppl. 63 (3), 1–14.
Merler, S., Ajelli, M., Fumanelli, L., Gomes, M.F.C., Pastore y Piontti, A., Rossi, L., Chao, D.L., Longini, I.M., Halloran, M.E., Vespignani, A., 2015. Spatiotemporal spread of the 2014 outbreak of Ebola virus disease in Liberia and the effectiveness of non-pharmaceutical interventions: a computational modelling analysis. Lancet Infect. Dis. 3099 (14), 1–8.
Moody, J., 2002. The importance of relationship timing for diffusion. Soc. Forces 81 (1), 25–56.
Morris, M., Kretzschmar, M., 1997. Concurrent partnership and the spread of HIV. AIDS 11 (5), 641–648.
Newman, M.E.J., 2002. Spread of epidemic disease on networks. Phys. Rev. E 66, 016128.
Ni, S., Weng, W., 2009. Impact of travel patterns on epidemic dynamics in heterogeneous spatial metapopulation networks. Phys. Rev. E 79 (1), 016111.
Nishiura, H., Chowell, G., 2014. Early transmission dynamics of Ebola virus disease (EVD), West Africa, March to August 2014. Eurosurveillance 19 (36), 20894.
Nyenswah, T.G., Westercamp, M., Kamali, A.A., Qin, J., Zielinski-Gutierrez, E., Amegashie, F., Fallah, M., Gergonne, B., Nugba-Ballah, R., Singh, G., Aberle-Grasse, J.M., Havers, F., Montgomery, J.M., Bawo, L., Wang, S., Rosenberg, R., 2014. Evidence for declining numbers of Ebola cases—Montserrado County, Liberia, June–October 2014, Morb. Mortal. Wkly. Rep., 63, 1–5.
Onnela, J.-P., Saramäki, J., Hyvönen, J., Szabó, G., Lazer, D., Kaski, K., Kertész, J., Barabási, A.-L., 2007. Structure and tie strengths in mobile communication networks. Proc. Natl. Acad. Sci. 104 (18), 7332–7336.
Pandey, A., Atkins, K.E., Medlock, J., 2014. Strategies for containing Ebola in West Africa. Science 16 (6212), 991–995.
Pastor-Satorras, R., Vespignani, A., 2001. Epidemic spreading in scale-free networks. Phys. Rev. Lett. 86, 3200–3203.
Pastor-Satorras, R., Castellano, C., Van Mieghem, P., Vespignani, A., 2015. Epidemic processes in complex networks. Rev. Mod. Phys. 87, 925–979.
Perra, N., Gonçalves, B., 2015. Modeling and predicting human infectious diseases. In: Gonçalves, B., Perra, N. (Eds.), Social Phenomena. From Data Analysis to Models. Springer International Publishing, Cham (ZG), Switzerland, pp. 59–83.
Perra, N., Balcan, D., Gonçalves, B., Vespignani, A., 2011. Towards a characterization of behavior-disease models. PloS One 6 (8), e23084.
Perra, N., Gonçalves, B., Pastor-Satorras, R., Vespignani, A., 2012. Activity driven modeling of time varying networks. Sci. Rep. 2, 469.
Poletti, P., Caprile, B., Ajelli, M., Pugliese, A., Merler, S., 2009. Spontaneous behavioural changes in response to epidemics. J. Theor. Biol. 260 (1), 31–40.
Poletto, C., Tizzoni, M., Colizza, V., 2013. Human mobility and time spent at destination: impact on spatial epidemic spreading. J. Theor. Biol. 338, 41–58.
Poletto, C., Gomes, M.F., Pastore y Piontti, A., Rossi, L., Bioglio, L., Chao, D.L., Longini, I.M., Halloran, M.E., Colizza, V., Vespignani, A., 2014. Assessing the impact of travel restrictions on international spread of the 2014 West African Ebola epidemic. Eurosurveillance 19 (42), 20936.
Rhee, I., Shin, M., Hong, S., Lee, K., 2011. On the Levy-walk nature of human mobility. IEEE/ACM Trans. Netw. 19 (3), 630–643.
Rivers, C., 2014. Data for the 2014 Ebola Outbreak in West Africa, ⟨https://github.com/cmrivers/ebola⟩.
Rivers, C.M., Lofgren, E.T.T., Marathe, M., Eubank, S., Lewis, B.L., 2014. Modeling the impact of interventions on an epidemic of Ebola in Sierra Leone and Liberia. PLoS Curr. 6, 1–16.
Rizzo, A., Frasca, M., Porfiri, M., 2014. Effect of individual behavior on epidemic spreading in activity driven networks. Phys. Rev. E 90, 042801.
Rizzo, A., Porfiri, M., 2016. Innovation diffusion on time-varying activity networks. Eur. Phys. J. B, 89 (1), 1–8.
Ruan, S., Wang, W., Levin, S.A., 2006. The effect of global travel on the spread of SARS. Math. Biosci. Eng. 3 (1), 205–218.
Scholtes, I., Wider, N., Pfitzner, R., Garas, A., Tessone, C.J., Schweitzer, F., 2014. Causality-driven slow-down and speed-up of diffusion in non-Markovian temporal networks. Nat. Commun. 5.
Schwartz, I.B., Shaw, L.B., 2010. Rewiring for adaptation. Physics 3, 17.
Shaw, L.B., Schwartz, I.B., 2010. Enhanced vaccine control of epidemics in adaptive networks. Phys. Rev. E 81, 046120.
Sousa da Mata, A., Pastor-Satorras, R., 2015. Slow relaxation dynamics and aging in random walks on activity driven temporal networks. Eur. Phys. J. B 88 (2), 1–8.
Starnini, M., Pastor-Satorras, R., 2014. Temporal percolation in activity-driven networks. Phys. Rev. E 89 (3), 032807.
Sun, K., Baronchelli, A., Perra, N., 2014. Epidemic spreading in non-Markovian time-varying networks, arXiv preprint, arxiv.org/abs/1404.1006.
Tang, J., Scellato, S., Musolesi, M., Mascolo, C., Latora, V., 2010. Small-world behavior in time-varying graphs. Phys. Rev. E 81, 055101.
The WHO Ebola Response Team, 2014. Ebola virus disease in West Africa—The first 9 months of the epidemic and forward projections. New Engl. J. Med. 371 (16), 1481–1495.
Towers, S., Patterson-Lomba, O., Castillo-Chavez, C., 2014. Temporal variations in the effective reproduction number of the 2014 West Africa Ebola outbreak. PLoS Curr. 6, 1–13.
Valdano, E., Ferreri, L., Poletto, C., Colizza, V., 2015. Analytical computation of the epidemic threshold on temporal networks. Phys. Rev. X 5 (2), 021005.
Valdez, L.D., Aragão Rêgo, H.H., Stanley, H.E., Braunstein, L.A., 2015. Predicting the extinction of Ebola spreading in Liberia due to mitigation strategies. Sci. Rep. 5, 12172.
van den Broeck, W., Gioannini, C., Gonçalves, B., Quaggiotto, M., Colizza, V., Vespignani, A., 2011. The GLEaMviz computational tool, a publicly available software to explore realistic epidemic spreading scenarios at the global scale. BMC Infect. Dis. 11 (1), 37.
Vespignani, A., 2011. Modelling dynamical processes in complex socio-technical systems. Nat. Phys. 8 (1), 32–39.
VirginiaTech Network Dynamics & Simulation Science and Laboratory, 2014. Modeling Updates, ⟨http://www.vbi.vt.edu/ndssl/ebola/modeling-view/modeling-the-ebola-outbreak-in-west-africa-august-11th-2014-update⟩.
Volz, E., Meyers, L.A., 2008. Epidemic thresholds in dynamic contact networks. J. R. Soc. Interface 6 (32), 233–241.
Wang, L., Zhang, Y., Huang, T., Li, X., 2012. Estimating the value of containment strategies in delaying the arrival time of an influenza pandemic: a case study of travel restriction and patient isolation. Phys. Rev. E 86 (3), 032901.

Webb, G., Browne, C., Huo, X., Seydi, O., Seydi, M., Magal, P., 2015. A model of the 2014 Ebola epidemic in West Africa with contact tracing. PLoS Curr. 7, 1–11.
World Health Organization, 2014a. Ebola Situation Reports, ⟨http://apps.who.int/ebola/en/current-situation/ebola-situation-report⟩.
World Health Organization, 2014b. Ebola Virus Disease, ⟨http://www.who.int/mediacentre/factsheets/fs103/en/⟩.
World Health Organization, 2015. The Ebola Outbreak in Liberia is Over, ⟨http://www.who.int/mediacentre/news/statements/2015/liberia-ends-ebola/en/⟩.
Yang Wang, W., Chakrabarti, D., Wang, C., Faloutsos, C., 2003. Epidemic spreading in real networks: an eigenvalue viewpoint. In: 2003 Proceedings of 22nd International Symposium on Reliable Distributed Systems, pp. 25–34.